STUDIA UBB CHEMIA, LXI, 3, Tom I, 2016 (p. 275-283)
(RECOMMENDED CITATION)

Dedicated to Professor Luminița Silaghi-Dumitrescu on the occasion of her 65th anniversary

ANTIMICROBIAL ACTIVITY OF CERAMIC DISKS LOADED WITH SILVER IONS AND NITROXOLINE

ANCUTA DANISTEAN[a], MARIA GOREA[a], ALEXANDRA AVRAM[a], SORIN RAPUNTEAN[b], GHEORGHE TOMOAIA[c], AURORA MOCANU[a], CORINA GARBO[a], OSSI HOROVITZ[a], MARIA TOMOAIA-COTISEL[a*]

ABSTRACT. Ceramic porous disks made of hydroxyapatite, HAP, loaded with silver ions and nitroxoline (5-nitro-8-hydroxyquinoline, NHQ) are used in vitro against pathogens, such as *Staphylococcus aureus*. HAP powder was synthesized by a wet chemical method, and its phase purity and nanocrystalline structure were assessed by X-ray diffraction (XRD), transmission electron microscopy (TEM) and atomic force microscopy (AFM). Disk samples of HAP were prepared and impregnated with Ag^+ ions and NHQ solutions. A strong antimicrobial activity of all samples was assessed by the diffusion assay in vitro against *Staphylococcus aureus.* Through the development of the optimal composition of these biomaterials, this approach might hold potential applications for antimicrobial coating, bone tissue engineering scaffolds and biomedical devices.

Keywords: *ceramics, hydroxyapatite, silver ions, 5-nitro-8-hydroxyquinoline, antimicrobial effect*

INTRODUCTION

Ceramics, such as nano crystalline hydroxyapatite, HAP, has been widely used as bone cement due to its structural similarity to inorganic component of natural bone and to its bone conductive properties. The HAP

[a] *Babeş-Bolyai University, Faculty of Chemistry and Chemical Engineering, 11 Arany Janos Str., RO-400028, Cluj-Napoca, Romania*
[b] *University of Agricultural Sciences and Veterinary Medicine of Cluj-Napoca, 3-5, Mănăstur Str., RO-400372, Cluj-Napoca, Romania*
[c] *Orthopedy and Traumatology Department, Iuliu Hatieganu University of Medicine and Pharmacy, 47 Traian Mosoiu Str., RO-400132 Cluj-Napoca, Romania*
** Corresponding author: mcotisel@gmail.com*

coatings of orthopedic implants are also used, particularly in hip surgery, to enhance the implant osseo-integration. Although the estimated risk is rather low (about 5%), the post-operative infections are still major cause of bone tissue damage and might lead to the removal of implants and consequently, to an increased cost of treatment. To reduce the implant derived infections, the localized delivery of antimicrobial compounds using HAP as a support is the best choice for the prevention of bone infections [1-4]. Due to increased antibiotic resistance, the alternative use of Ag^+ or silver nanoparticles, alone or in combination with antibiotics, is recommended [5-13]. 5-Nitro-8-hydroxyquinoline (nitroxoline: NHQ) [14] is a broad-spectrum antimicrobial agent, used as urinary antibiotic [15]. It is practically insoluble in water, at room temperature, but soluble in organic solvents [16]. At 298 K, the mole fraction, x, of NHQ in its saturated solution in ethanol is x = 0.0018 [16], which corresponds to a 0.02 M solution (3.8 g NHQ/L).

This investigation is focused on the antimicrobial effect of nitroxoline and of silver nitrate, and on the possible interaction of Ag^+ and NHQ leading to supramolecular associations, which could modulate their biological activity. They are adsorbed on HAP disks, which possess an enhanced adsorptive ability both for Ag^+ and for biomolecules, such as nitroxoline. Their antimicrobial effectiveness is assessed by Kirby-Bauer diffusion assay [17] on agar plates, against *Staphylococcus aureus* microbial strain.

RESULTS AND DISCUSSION

Characterization of HAP powders. Two synthesized HAP powders are used, namely HAP1 calcined at 450 ^oC and HAP2 further calcined at 850 ^oC. The XRD patterns are similar for HAP1 and HAP2 and show only the characteristic peaks for pure HAP indicating a unique phase of stoichiometric HAP of high phase purity. As an example XRD patterns for HAP2 are given in Fig. 1. The average crystallite size estimated by the Debye-Scherrer method is about 49.6 nm (HAP1) and 60.3 nm (HAP2), while the crystallinity degree for HAP1 is about 64.8% and for HAP2 is rather high, around 78.5 %.

TEM images for HAP2 are given in Fig. 2, together with the histogram obtained by measuring the diameters of a large number of particles. The average diameter of HAP2 particles is of 65.1 ± 17.0 nm.

A representative example of AFM images is given in Fig. 3 and confirms this size of HAP2 particles, about 67 ± 5 nm.

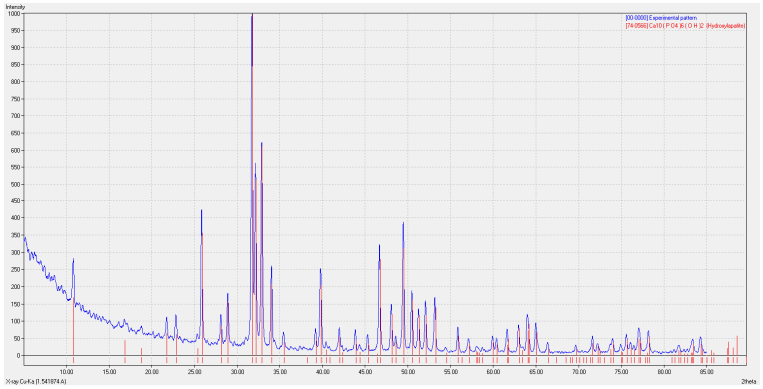

Figure 1. XRD patterns for the synthesized HAP2 powder compared with PDF 74-0566 for stoichiometric hydroxyapatite

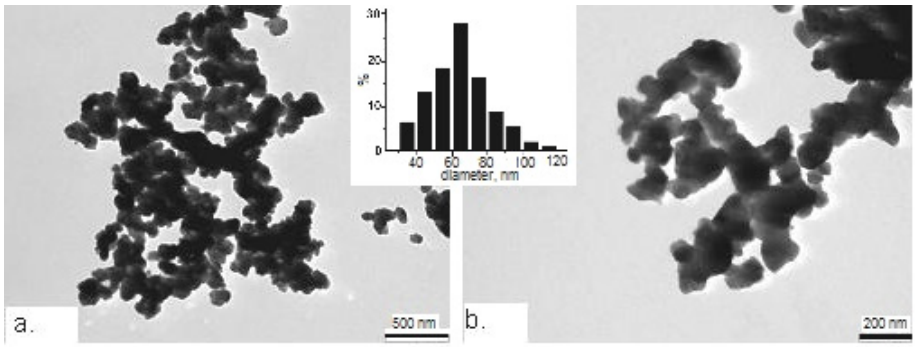

Figure 2. TEM images for HAP2 particles and histogram of their size distribution. The bars in the TEM images are 500 nm (a), and 200 nm (b).

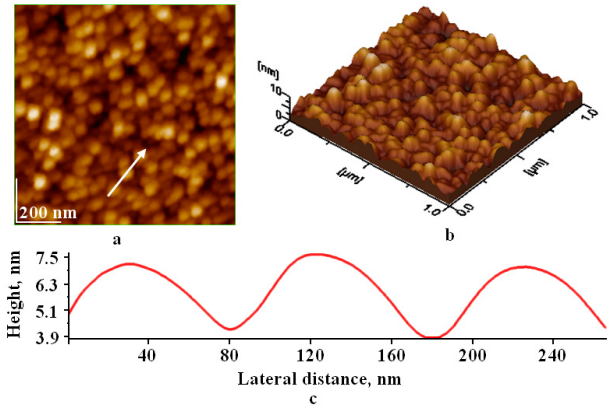

Figure 3. AFM images for HAP2 adsorbed on glass for 10 s from aqueous dispersion: (a) 2D-topographical image; (b) 3D-topographical image; (c) cross section profile along the arrow in panel (a); scanned area: 1 μm x 1 μm

Characterization of ceramic disks. Compactness characteristics of the sintered disk ceramics were determined using air and water weight method. Apparent density, ρ_a, water absorption, a_m, and apparent porosity, P_a, were determined (Table 1). The apparent porosity of ceramic disks is high. This property allows various solutions to penetrate within porous disks, and give an optimal choice for disk adsorption of the components from solutions. Consequently, active silver ions and NHQ biomolecules, impregnated into HAP disks, can be released into microbial medium.

Antimicrobial activity. In Fig. 4 are presented representative images of the agar plates with *Staphylococcus aureus* cultures after incubation at 37°C for 24 hours, with ceramic disks (Fig. 4a) and with the initial solutions in which the disks had been immersed (Fig. 4b). The diameters of the inhibition zones, in mm, are given in Table 2.

Table 1. Characteristics of the ceramic disks

Ceramic disks	Sample No	Apparent density, ρ_a [%]	Water absorption, a_m [%]	Apparent porosity, P_a [%]
HAP1	1	1.24	38.27	47.67
	2	1.36	34.41	47.01
	3	1.46	37.31	54.73
HAP2	1	1.57	29.44	46.39
	2	1.31	36.70	48.12
	3	1.21	36.63	44.56

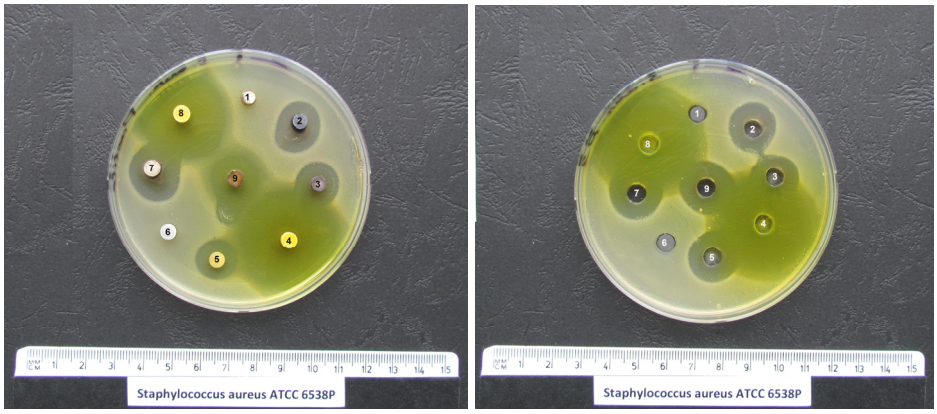

a. b.

Figure 4. Inhibition zones for *Staphylococcus aureus* in presence of ceramic disks loaded with antimicrobial solutions (a), or in presence of antimicrobial solutions in wells (b). Samples are numbered as follows: 1 for HAP1/water and 6: HAP2/water, each as control; 2 and 3: HAP1/$AgNO_3$; 7: HAP2 /$AgNO_3$; 4: HAP1/NHQ; 8: HAP2/NHQ; 5: HAP2/NHQ + $AgNO_3$; 9: HAP1/NHQ + $AgNO_3$.

Table 2. Inhibition zones for the samples presented in Fig. 4; the labels are the same as in Fig. 4

	Inhibition zones (mm)								
Samples	1	2	3	4	5	6	7	8	9
Disks	-	15	15	>30	14	-	17	>30	18
Solutions	-	18	18	>30	17	-	18	>30	18

The control disks, samples 1 and 6 (HAP1, HAP2, in pure water) did not produce any inhibition zone. The largest effect is observed for disks loaded with NHQ, sample 4 (HAP1) and sample 8 (HAP2) (Fig. 4a), and for their corresponding NHQ solutions, which remained after removing the disks (at about 24h from preparation) for antimicrobial evaluation (Fig. 4b). The antimicrobial effect of the NHQ impregnated HAP1 disk (sample 4) was very strong (> 30 mm) and comparable with that of the sample 8, HAP2/NHQ. It is clear evidence that NHQ adsorbed and incorporated into ceramic disks has a strong effect on *S. aureus.* The antimicrobial effect of ceramic disks loaded with NHQ is also comparable with that of NHQ solutions (samples 4 and 8, in Fig. 4b) showing that *S. aureus* is highly susceptible in vitro to NHQ. The Ag^+ ions loaded disks (Fig. 4a) and their corresponding $AgNO_3$ solutions (Fig. 4b), namely samples 2, 3 and 7 also show distinct inhibition zones. The antimicrobial effect of Ag^+ loaded HAP1 disk (samples 2 and 3, Fig. 4a) is smaller than that corresponding to the Ag^+ solutions (Fig. 4b). The cause might be the interaction of Ag^+ with the surface of ceramic nanoparticles within the disk leading to a retard delivery of Ag^+. However, the inhibition zone is almost the same (Table 2) for HAP2 disk loaded with Ag^+ (sample 7, Fig. 4a) and for Ag^+ in solution (sample 7, Fig. 4b). This shows that characteristics of HAP disks are also important.

The antimicrobial effect (Table 2) for HAP1 disk (sample 9) previously immersed in the initial NHQ solution for 30 min, is higher than that of HAP2 disk immersed for 15 min (sample 5), both immersed after removing from NHQ, in 5 mL 10^{-2} M $AgNO_3$ solution each. The effect of the disk sample 5 (14 mm) is lower than that for its corresponding solution, sample 5 in Fig. 4b (17 mm, Table 2). On the other hand, the antimicrobial effect of the disk sample 9 is the same as that of its corresponding solution (Table 2), showing the importance of adsorption time of biomolecules on ceramic disks to reach adsorption equilibrium. This situation is more complex and shows also the importance of the self-assemblies of NHQ and Ag^+, adsorbed on ceramic disks as well as their role in antimicrobial activity. Specifically, the antimicrobial effects of $AgNO_3$ solutions, samples 5 and 9, are almost the same as those for samples 2, 3 and 7, showing in fact the effect of pure $AgNO_3$ solution, since this was the final solution around ceramics disks impregnated with NHQ (samples 5 and 9).

The results are in substantial agreement with earlier results [17] showing discrete inhibitory effects characteristic for an investigated system.

CONCLUSIONS

This investigation demonstrates the antimicrobial effect of nitroxoline (NHQ), Ag^+ and their self-assemblies or clusters against *Staphylococcus aureus* in vitro, under given experimental conditions. Results demonstrate for the first time the ability of NHQ and of Ag^+ to diffuse from ceramic disks and to exert their antimicrobial effect. This technique of self-assembly on ceramic disks uses as a driving force for surface adsorption, electrostatic and van der Waals interaction, as well as hydrogen bonding and hydrophobic interaction [24, 25]. It offers another approach to depositing antimicrobial agents, such as NHQ and silver ions, within ceramics disks for their local retard delivery with potential applications to prevent or to treat infections. Further studies are needed to evaluate the efficacy of NHQ and silver ions impregnated ceramic disks against *S. aureus*. This investigation can be extended to various pathogens to explore the possible applications of NHQ and Ag^+ incorporated in ceramic disks to address the susceptibility of microbial biofilms.

EXPERIMENTAL SECTION

Preparation of HAP powders. A chemical precipitation method was applied [17-23]. A 0.25 M calcium nitrate solution was obtained from $Ca(NO_3)_2 \cdot 4H_2O$ (pure p.a., Poch S.A., Gliwice, Poland) dissolved in ultrapure water, with 25% ammonia solution, pH value 8.5, and o-toluidine p.a. (Merck) as template. A second solution was a 0.15 M diammonium hydrogen phosphate ($(NH_4)_2HPO_4$ pure p.a., SC Nordic Invest SRL, Romania) solution in ultrapure water, with 25% NH_3 solution, pH 11 and ethylene diamine (EDA, from Merck) as template. Equal volumes of the two solutions, at 22°C, were quickly mixed using a peristaltic pump (Masterflex L/S Digital Drive, 600 RPM, 115/230 VAC, EW-07523-80) and an impact reactor type Y for the two fluid streams, with the reactants in stoichiometric molar ratio Ca/P = 1.67. A maturation treatment was applied to the obtained suspension (70°C, 24 h). To avoid agglomeration of particles during further processing, they were coated with urea-formaldehyde (UF) resin prepared *in situ* from an aqueous 30% CH_2O solution and urea in a 1.5 mole ratio, final pH 8.5. After maturation (85-95°C, 8 h) the precipitate was filtered (Filter Disks Munktell, grade: 382), washed with ultrapure water (until free of nitrate ions) and dried by

lyophilization. Thus obtained material was dispersed in a colloidal mill, for 2 h and calcined 4h at 450 ºC, in order to burn the organic matter (HAP1 powder); and further for another 4 h at 850ºC, for HAP2 powder, with increased crystallinity.

Physical characterization methods. X-ray diffraction (XRD) patterns were obtained using a DRON-3 diffractometer, in Bragg–Brentano geometry, having a X-ray tube with copper K_α radiation, wave-length 1.541874 Å). Phases were identified by comparing the peak positions with PDF (Powder Diffraction File) 74-0566 for stoichiometric hydroxyapatite. HAP aqueous dispersions needed for TEM and AFM imaging were prepared by ultra-sonication (Sonics Vibra-Cell, model VCX 750), for 5 min, at 22°C. TEM images obtained with TEM, JEOL – JEM 1010 equipment have been recorded with JEOL standard software. The AFM JEOL 4210 equipment was operated in tapping mode [26], using standard cantilevers with silicon nitride tips. The particles were adsorbed (vertical adsorption) from their aqueous dispersion for 10 s on glass. Different areas from 10 µmx10 µm to 0.5 µmx0.5 µm were scanned on the same HAP layer. The AFM images (2D- and 3D-topographies) and cross-section profiles for the adsorbed HAP layer, along a selected direction were processed by the standard AFM JEOL procedures.

***Preparation of ceramic disks*.** The HAP powder was mixed with a 2 % polyvinyl alcohol solution as a binding material for granulating and obtaining a final powder humidity of 6%. The ceramic disks with 6 mm diameter and 3 mm in height were pressed at 1000 kgf/cm^2. The raw HAP disks were dried in a laboratory oven at 100 ºC. Dried ceramic disks were sintered in air at 900 ºC in a laboratory kiln using a 5 ºC/min heating rate and a plateau at the maximum temperature of one hour.

Antimicrobial activity assessment. The HAP1 and HAP2 disks were treated by immersing each in 5 mL of the following solutions: ultrapure water (witness samples 1 (HAP1) and 6 (HAP2); 10^{-2} M $AgNO_3$ (Merck, Germany) solution: samples 2 and 3 (HAP1), and 7 (HAP2); saturated NHQ (Sigma-Aldrich, Germany) solution in ethanol (sample 4: HAP1, and sample 8: HAP2); NHQ solution for 15 min (HAP2, sample 5), and for 30 min (HAP1, sample 9) and then moved in $AgNO_3$ solution. The tested microbial strain was *Staphylococcus aureus* 6538P ATCC. It was streaked on glucose medium (nutrient broth and agar) (TM MEDIA, TITAN BIOTECH, India). The inhibitory effect was determined by Kirby-Bauer technique [17] (agar diffusion test). The nutrient agar, after liquefaction by heating on a water bath, was poured in Petri dishes (diameter of 90 mm) in an amount of 25 ml to form a uniform layer with about 3 mm thick. Inoculation was done by flooding, using 1 ml suspension

of the test strain at a density of 0.5 (according to "McFarland Standards"). The agar surface was dried in the incubator for 20 min with the lid slightly open. After 24h, the disks were removed from the liquid using a tissue plier DeBakey, previously sterilized in open flame and cooled in sterile distilled water. Disks were radially placed on the agar plate. On another plate, wells (ø = 6 mm) were cut in the agar gel, also by a radial pattern, and 20 µL of the liquid in contact with the disks was put in each well. The plates were incubated at 37°C for 24 h, and then the presence or absence of *S. aureus* culture development around the disks or wells was assessed. In the case of an inhibitory effect, the diameter of the inhibition zones was measured. The plates were further maintained under observation for an extra 5 days.

ACKNOWLEDGMENTS

The authors acknowledge funding by the UEFISCDI through the grants no. 171 and 257.

REFERENCES

1. M. Vukomanović, I. Bračko, I. Poljanšek, D. Uskokovič, S.D. Škapin, D. Suvorov, *Crystal Growth & Design*, **2011**, *11*, 3802.
2. L. Yang, X. Ning, Q. Xiao, K. Chen, H. Zhou, *Journal of Biomedical Materials Research*, *Part B*, **2007**, *81B*, 50.
3. B. Xiao, M. Karren, M.R. Christopher, A. Rabiei, *Acta Biomaterialia*, **2010**, *6*, 2264.
4. V. Stanic, D. Janackovic, S. Dimitrijevic, B.S. Tanaskovic, M. Mitric, S.M. Pavlovic, A. Krstic, D. Jovanovic, S. Raicevic, *Applied Surface Science*, **2011**, *257*, 4510.
5. P.N. Lim, L. Chang, E.S. Thian, *Nanomedicine*, **2015**, *11*, 1331.
6. W.K. Jung, H.C. Koo, K.W. Kim, S. Shin, S.H. Kim, Y.H. Park, *Applied and Environmental Microbiology*, **2008**, *74*, 2171.
7. Q.L. Feng, J. Wu, G.Q. Chen, F.Z. Cui, T.N. Kim, J.O. Kim, *Journal of Biomedical Materials Research*, **2000**, *52*, 662.
8. I. Chopra, *Journal of Antimicrobial Chemotherapy*, **2007**, *59*, 587.
9. S.H. Kim, H.S. Lee, D.S. Ryu, S.J. Choi, D.S. Lee, *Korean Journal of Microbiology and Biotechnology*, **2011**, *39*, 77.
10. A.R. Shahverdi, A. Fakhimi, H.R. Shahverdi, S.Minaian. *Nanomedicine: Nanotechnology, Biology, and Medicine*, **2007**, *3*, 168.
11. A.M. Fayaz, K. Balaji, M. Girilal, R. Yadav, P.T. Kalaichelvan, R. Venketesan, *Nanomedicine: Nanotechnology, Biology, and Medicine*, **2010**, *6*, 103.
12. W. Suvannapruk, F. Thammarakcharoen, P. Phanpiriya, J. Suwanprateeb, *Journal of Nanomaterials*, **2013**. Article ID 542584, 9 pages http://dx.doi.org/10.1155/2013/542584

13. J.R. Morones-Ramirez, J.A. Winkler, C.S. Spina, J.J. Collins, *Science Translational Medicine*, **2013**, *5*, 190ra81.
14. V.G. Voronin, I.D. Petrova, A.N. Leksin, B.V. Shemeryankin, *Pharmaceutical Chemistry Journal*, **1976**, *10*, 1215.
15. A. Sobke, M. Klinger, B. Hermann, S. Sachse, S. Nietzsche, O. Makarewicz, P.M. Keller, W. Pfister, E. Straube, *Antimicrobial Agents and Chemotherapy*, **2012**, *56*, 6021.
16. Y. Cong, J. Wang, C. Du, S. Han, L. Meng, H. Zhao, *The Journal of Chemical Thermodynamics*, **2016**, *100*, 60.
17. A. Mocanu, G. Furtos, S. Răpunţean, O. Horovitz, C. Flore, C. Garbo, A. Dănişteanu, G. Răpunţean, C. Prejemrean, M. Tomoaia-Cotisel, *Applied Surface Science*, **2014**, *298*, 225.
18. C. Garbo, M. Sindilaru, A. Carlea, Gh. Tomoaia, V. Almasan, I. Petean, A. Mocanu, O. Horovitz, M. Tomoaia-Cotisel, *Particulate Science and Technology,* **2015***,* DOI:10.1080/02726351.2015.1121180.
19. Gh. Tomoaia, A. Mocanu, L.-D. Bobos, L.-B. Pop, O. Horovitz, M. Tomoaia-Cotisel, *Studia UBB Chemia*, **2015**, *60(3)*, 265.
20. Gh. Tomoaia, M. Tomoaia-Cotisel, L. B. Pop, A. Pop, O. Horovitz, A. Mocanu, N. Jumate, L.-D. Bobos, *Revue Roumaine de Chimie*, **2011**, *56*, 1039.
21. Gh. Tomoaia, L.B. Pop, I. Petean, M. Tomoaia-Cotisel, *Materiale Plastice*, 49 (1), 48-54 (2012).
22. Gh. Tomoaia, O. Soritau, M. Tomoaia-Cotisel, L.-B. Pop, A. Pop, A. Mocanu, O. Horovitz, L.-D. Bobos, *Powder Technology*, **2013**, *238*, 99.
23. Gh. Tomoaia, A. Mocanu, I. Vida-Simiti, N. Jumate, L. D. Bobos, O. Soritau, M. Tomoaia-Cotisel, *Materials Science and Engineering C*, **2014,** *37*, 37.
24. X. Wei, M. Luo, H. Liu, *Colloids and Surfaces B: Biointerfaces,* **2014**, *116*, 418.
25. B. Zhou, Y. Li, H. Deng, Y. Hu, B. Li, *Colloids and Surfaces B: Biointerfaces,* **2014**, *116*, 432.
26. O. Horovitz, Gh. Tomoaia, A. Mocanu, T. Yupsanis, M. Tomoaia-Cotisel, *Gold Bulletin*, **2007**, *40*, 295.